Nanomaterial SnS$_2$-Based Sensor
for VOC Gas Detection at Room Temperature

To Thi Nguyet[1], Dang Thanh Binh[3],
Chu Manh Hung[1,2], Jian Zhen Ou[4], Nguyen Duc Hoa[1,2]*

[1]*International Training Institute for Materials Science (ITIMS),*
Hanoi University of Science and Technology Ha Noi, Vietnam
[2]*School of Materials Science and Engineering, Hanoi University of Science and Technology, Ha Noi, Vietnam*
[3]*Center for High Technology Research and Development,*
Vietnam Academy of Science and Technology, Ha Noi, Vietnam
[4]*School of Engineering, RMIT University, Melbourne, Victoria, Australia*
**Corresponding authors email: ndhoa@itims.edu.vn/hoa.nguyenduc@hust.edu.vn*

Abstract

Real-time indoor hazardous gases monitoring has gained interest in ensuring human health. An effort to design gas sensing devices, which are compact in size, flexible, and low power consumption, providing high-performance sensing plays a crucial role in precise sensing of the indoor environment. Here, we have fabricated 2D SnS$_2$ flakes for gas sensor. The 2D ultra-thin SnS$_2$, including a few layers, shows fascinating sensing toward Volatile organic compounds (VOCs) under room temperature with high response and fast reaction speed. The short-term stability versus time of the SnS$_2$ sensor is investigated. Due to the great adsorption of gaseous molecules, the SnS$_2$-gas sensor operates at room temperature without external heating sources. The Schottky junction-based sensor is one of the key factors contributing to the higher performance of the sensor. Furthermore, its VOC-sensing mechanism is explained obviously through the energy band diagram. The SnS$_2$-layer is considered a promising candidate in indoor VOCs monitoring and respiratory biomarker analysis in the future.

Keywords: SnS$_2$ flakes, VOCs gas, room temperature, 2D materials.

1. Introduction

Detection of Volatile organic compounds (VOCs) are essential due to its presence in various applications. The last time, the ongoing coronavirus disease 2019, which is known as the COVID-19 epidemic of the 20th century, killed over two and a half million patients worldwide [1]. Diagnosis of COVID 19 relies main on the clinical symptoms (namely cough, headache, myalgias, sore throat, smell or taste abnormalities) blood, and polymerase chain reaction testing [2,3]. These testing methods demand sophisticated equipment, high technician, complicated sample preparation, and high cost. Exhaled breath analysis is an alternative approach, especially the evaluation and separation of VOCs gases contained in human breath have attracted notable study. Some volatile gases observed in COVID-19 patients were methylpent-2-enal, 1-chloroheptane, and nonanal [4]. In addition, there are thousands of different volatile organic compounds produced from the metabolic processes in the human body [5], for instance, acetone is used as a biomarker for diabetes detection in case concentration excess of 1.8 ppm meanwhile its concentration in exhaled breath from the normal individual is lower than 0.8 ppm [5, 6].

In addition, air pollution is a serious issue due to rapid industrialization, meanwhile humans are facing an increasing continuous number of patients from COVID -19 epidemic. One of the pollutant gases being introduced into the environment consists of hazardous gases such as CO, NO$_2$, SO$_2$, and VOCs. According to the WHO, both outdoor and indoor air pollution is responsible for about 7 million deaths globally each year [7]. The fact revealed that indoor pollution levels occupied much ten times higher than outdoor ones which are researched by the United States Environmental Protection Agency because of long time exposure of people to toxic gases in households [8] such as schools, hospitals, factories, and offices. Among toxicants, the chemical total volatile organic compounds class is the primary contributor to poor air quality. Ethanol and Acetone, classical chemical elements of alcohols and ketones, are significant health hazards associated with exposure even low-concentration [9]. These VOCs are attributed to an industrial cleaning agent, PVC cement and primer, and various adhesives. The presence of toxic gases can be harmful to the nervous and immune systems. There

were 3.8 million people faced with illnesses (e.g, headache, damage to the liver, kidney, central nervous system, and lung cancer), and nearly 20% of cardiovascular deaths were related to household pollution [10]. Therefore, to ensure the level of safety in the household, it is crucial to develop novel electronic devices that determine the gaseous concentration and distinguish between these in many VOC gas mixtures.

The resistive gas sensor is a potential candidate in sensing applications owing to its great sensing characteristics, compact size, and low-cost compared to user devices. Up to now, the chemiresistive sensor based on metal oxide semiconductor (MOS) sensing material shows the merits of reliable and stable sensing performances, as well as high response in a short time. However, there is the remaining disadvantage, consisting of high temperature (>150 °C), poor selectivity, and difficulty to meet the detection limit in exhaled breath (sub ppb) thus it hinders their potential in the different applied fields [11].

An effective approach is seeking novel material, which shows promising characteristics. Recently, two-dimensional 2D materials show fascinating properties, for instance, graphene and its derivative are developed into VOCs gas, but the absence of an electronic bandgap has prevented research. Finding other 2D materials with semiconducting features is essential to enhance gas absorption rate. An effort in this process revealed transition-metal dichalcogenides (TMDCs) being semiconducting metal atoms, which denotes an MX2 structure whereas M denotes transition metal atoms (such as Mo, W, Ti, etc.) and X denotes a chalcogen atom (such as Se, Te, S) [12]. The TMD material has been studied in various applications such as optoelectronics, flexible electronics, energy harvesting, and gas sensor owing to its unique electronic, optical, and mechanical properties and direct bandgap structure [13, 14].

Among these metal sulfides, tin disulfide (SnS_2) is a 2D nanostructure with desirable properties such as narrow band gap (E_g=2.3 eV), larger electronegativity, and large surface to volume ratio [15], making the SnS_2-sensor more suitable for the start-of-art devices like portable instruments, E-nose and sensor array. Till now, the number of publications of SnS_2 nanomaterial related to VOCs discrimination under low temperatures is few. For example, Yang Lu [16] *et al.* reported that Au-Pd nanoparticles were modified on their surface of SnS_2 using reducing agents. The AuPd-SnS_2 gas sensor exhibited excellent xylene-sensitive properties owing to the synergistic effect of the bimetal and the catalytic properties of bimetallic systems. A potential approach is a combination of SnS_2 nanosheets with MoO_3 in detecting triethylamine [17]. The sensor based on α-MoO_3@SnS_2 shows a high response of 114.9 exposure to 100 ppm triethylamine

at working temperature 175 °C and wide concentration detection range (500 ppb to 500 ppm). To enhance the selective properties of ethanol, Zhang and his co-author [18] successfully synthesized SnS/SnS_2 heterojunction via one-step hydrothermal treatment. The response of SnS/SnS_2 nanoparticles to 100 ppm reaches 30.12 at 200 °C, which is 1.64 times higher than that of pure SnS_2. In this research, the gas sensor, using pure SnS_2 or composite with SnS_2 as sensing layer, operates almost excess 200 °C leading to consumption of plenty of power.

Herein, the ultra-thin SnS_2 sheets consist of few-layered thickness were synthesized by wet chemical process for VOC gas sensor application. Accordingly, the sensing performance of SnS_2 toward VOCs (e.g, ethanol, acetone) was deeply investigated. We pointed out that the fabricated SnS_2 flakes exhibited excellent sensing performance for VOCs at room temperature. Furthermore, the sensing mechanism was discussed via energy band structure after introducing/exhausting the VOCs to the measuring chamber.

2. Experiment

Materials used in this works were tin (IV) chloride (>99.9%, Sigma-Aldrich), oleic acid (>90.0%, Sigma-Aldrich), octadecene (>90.0%, Sigma-Aldrich), oleylamine (>90.0%, Sigma-Aldrich).

The 2D SnS_2 flakes were prepared by a wet chemical method [19]. First, 0.5 mM of tin (IV) chloride, 5 mL oleic acid, and 10 mL of octadecene were mixed in a 100 mL three-neck flask while degasses were done by flowing the pure N_2 gas through the flask for 60 mins to eliminate the interference of oxygen and moisture. Then, the temperature of the solution was increased to 280 °C, and followed by vigorously stirring mixture about 15 mins to obtain the homogenous solution. After that, 1 mM pre-dispersed sulfide precursor in 5 mL of oleylamine was injected into the flask for further reaction. After about 15 mins, the solution was cooled to room temperature. The SnS_2 nanoflake powders were washed with ethanol and collected by separating them from the solution using centrifugation. Finally, the produces were dried in an electric oven for 24 hours at 60 °C.

The gas sensor was prepared by a facile drop-casting method at room temperature. First, the as-synthesized SnS_2 powders were dispersed in the ethanol solution to form a colloidal solution and then deposited in a thin layer on the interdigitated Au electrodes by micropipette. After instilling about 2-3 drops of SnS_2 solution on the electrode, this electrode would be placed on a heating plate and kept at about 100 °C to evaporate all the ethanol solvent. The resistance of the SnS_2-based sensor was measured by the digital meter at approximately 50 MΩ.
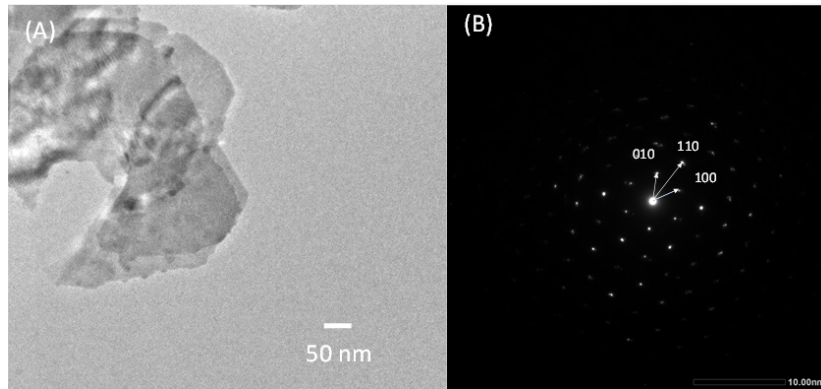
Fig. 1. (A) HRTEM image and (B) SAED of the fabricated SnS_2 flakes.

To record the changing electrical signal, the digital multimeter (Keithley 2602) was used. Details about the gas sensing measurement system were reported in our previous publication [20]. The dynamic response versus time of the sensor was determined by the ratio of R_a/R_g (for reducing gas), where R_a and R_g stand for the electrical resistances of the sensor in air and the target gas, respectively.

3. Results and Discussion

3.1. Material Characterization

The synthesized SnS_2 materials were characterized by high resolution transmission electron microscopy (HRTEM) image, and selected area electron diffraction (SAED) as shown in Fig. 1 (A-B). The flakes have a lateral dimension of about 500 nm with ultrathin morphology which is observed by dark gray region. The luminous diffraction spots obtained from Fig. 1 (B) indicate the well-defined crystalline structure with typical lattice structure (010), (110), and (100), characterizing for single crystallinity of SnS_2 hexagonal-liked nanosheets [21, 22].

The morphology of the fabricated sensor was studied by scanning electronic microscopy (SEM) image as shown in Fig. 2. Here, the electrode finger, and the gap between electrode fingers is approximately 10 µm. The gas sensing layer was thin; thereby, it would not likely see the SnS_2 flakes in the SEM image. Anyhow, we tested the resistance of the sensor at room temperature, which was about 50 MΩ.

Additionally, to confirm the formation of SnS_2 material, energy-dispersive X-ray (EDX) instrument experimented analysis of elemental composition and their percentage, as shown in Fig. 2 (B). It is observed the presence of two prominent elements, including S and Sn without other element, with atomic proportion of 68.33 and 31.67 %, respectively, which correspond the S and Sn atomic ratio is 2:1. These results indicate a thin layer of SnS_2 flakes was successfully deposited on the substrate for the gas sensor
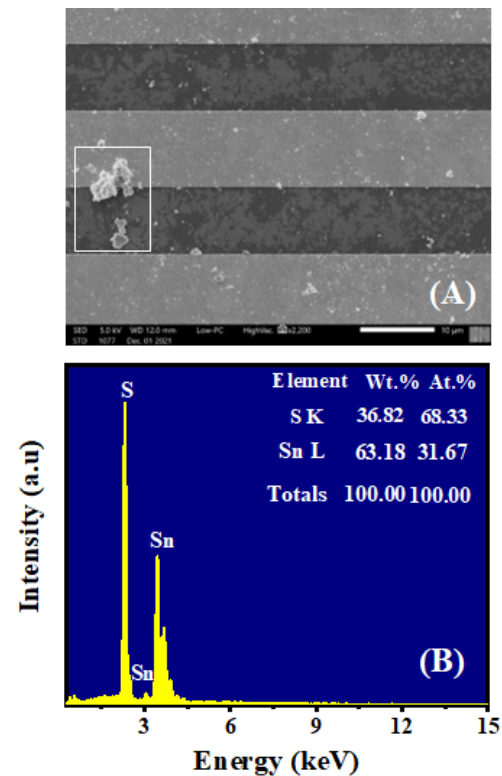

Fig. 2. SEM image of the prepared SnS_2 gas sensor (A) and EDX spectrum at the rectangular remarked region.

3.2. Electrical and Gas Sensing Characteristic of SnS_2 Nanosheets - Based Gas Sensor

The electrical characteristic of the sensor was analyzed by measuring the *I-V* curve at room temperature at an applied voltage between -5 V and 5 V, as shown in Fig. 3. The *I-V* characteristic indicates a Schottky contact between the SnS_2 and the Au electrodes. Furthermore, to demonstrate the repeatability of SnS_2-based gas sensor, five sensors are fabricated simultaneously and investigated electrical properties in similar testing condition. As shown in the figure, sensors indicate the non-linear characteristics with forward voltage of approximately 2 V.
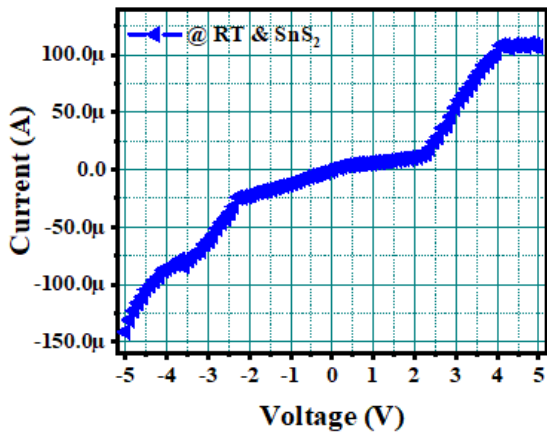
Fig. 3. I-V characteristic of the SnS_2 based sensor at room temperature in dried air.

The ultra-thin SnS_2 nanosheets with a high surface-to-volume ratio are expected to show great sensing performance under room temperature condition. Here, we tested the VOC gas sensing properties of the fabricated sensor at room temperature.

Fig. 4 (A) illustrates the dynamics of the resistance of the SnS_2 sensor to the various concentrations of 50, 100, 125, 250, 500, and 1000 ppm at room temperature. The wide range detection is greatly suitable for indoor safety quantity observation due to the acetone detection limits of 250 ppm according to the National Institute for Occupational Safety and Health (NIOSH) [23]. The resistance of the gas sensor tends to decrease upon exposure to acetone and return to its initial resistance after removing the target gas. Its curve shows n-type semiconductor behavior due to the reducing nature of acetone. The response value of the sensor is calculated in Fig. 4(B). It is noted that the response decreases with decreasing the acetone concentration. At room temperature, the response reaches a value of larger 5 times when the concentration is up to 1000 ppm. Meanwhile, its value is only 1.5 times upon exposure to 50 ppm. The fitting curve exhibits a linear relationship between the response signal and acetone contents, which is the best fit to a series of obtained response points for gas sensing even though the sensor absorbed the number of gases in the long range. In addition, the limit of detection (LOD) was extracted from the fitting line, as following equation [24]:

$$LOD = 3x \frac{rms_{noise}}{Slope} \qquad (1)$$

where rms_{noise} is the root - mean - square standard deviation of the noise in the response curve, the slope value was obtained from linear line of calibration curve. The acetone detection concentration reaches 12 ppm.
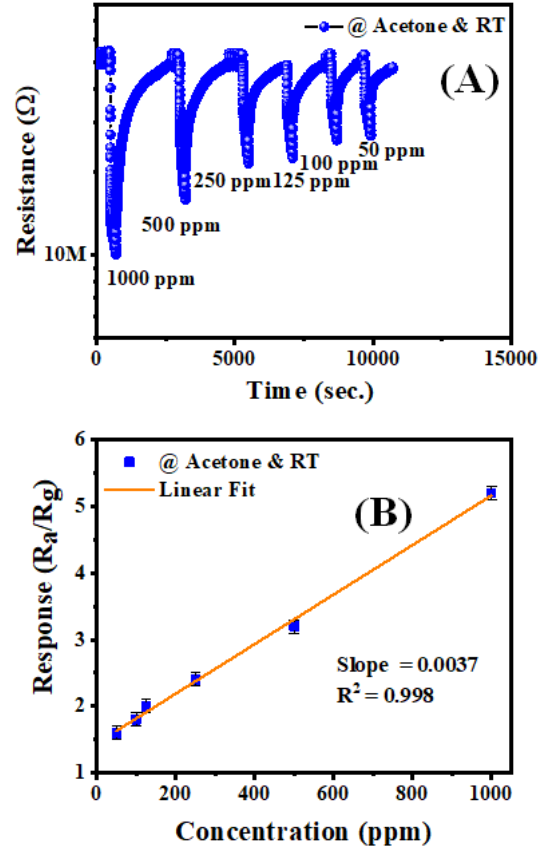

Fig. 4. Dynamic behavior of the resistance of the gas sensor (A), and response curve as a linear function to various acetone concentration at RT.

The sensing properties of ethanol were studied in this work. To understand the adsorption/desorption of ethanol gas and the chemical reaction on the surface of the SnS_2 nanosheet, the sensor is tested to ethanol gas at room temperature. Fig. 5(A) exhibits the dynamic resistance curve of the sensor to different concentrations in the range of 50 - 1000 ppm. It is easy to observe that the resistance modification of the sensor increases along with the increase of ethanol concentration. At the highest concentration, the resistance decreases from 25.2 MΩ to 0.5 MΩ, whereas its resistance is only down to 1.5 MΩ. The responses value to 50, 100, 125, 250, 500, and 1000 ppm of ethanol are about 15, 19, 27, 32, 44, 49, respectively. From Fig. 5(B), it is worth mentioning that the response value increased non-linearly with the ethanol concentration. The graph shows the exponential fitting, which is attributed to Langmuir adsorption theory [25], indicating the physisorption model. The response and recovery time of the SnS_2 sensor at different ethanol concentrations are indicated in Fig. 5 (C). The response time of the SnS_2 sensor decreases gradually versus investigated concentration, however, it is found out a reversible phenomenon in the recovery time. In detail, the sensor only required 118 s to respond and 602 s to recover when exposed to 1000 ppm, whereas its value is 211 s and 425 s upon 50 ppm ethanol, respectively.
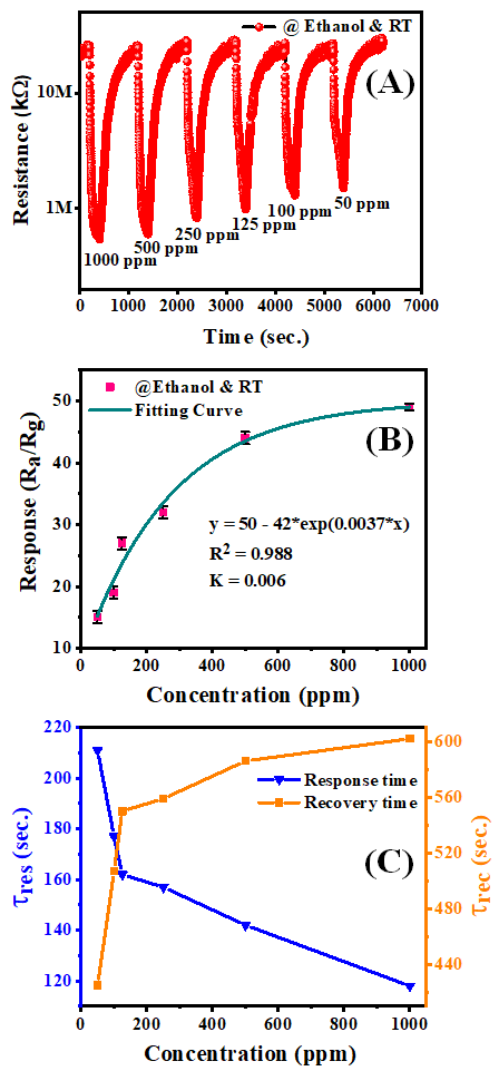
The sensor performance comparison between our sensors and recently reported in the scientific literature with sensors based on TMD material including MoS_2, $MoSe_2$, and WS_2 and their composites for sensing VOCs gas, are summarized in Table 1. It is confirmed that the SnS_2 sensor in this paper has fascinating gas sensing properties with low temperature and high sensitivity, as well as excellent selectivity toward ethanol. While the TMDs-based resistive sensors operate at high temperatures and lower sensitive signals.

One of the vital parameters to ensure the accuracy of the sensor in real-time monitoring is the repeatability and the stability of the sensor response.

In this study, we measured short-term sensitivity after nine continuous cycles turn on/off ethanol gas at room temperature. From Fig. 6, the sensor repeats well in terms of response and recovery. The recorded signal between each cycle is not significantly different and there is no sign of attenuation. From this point, the as-prepared SnS_2 sensor shows excellent repeatability. One of the vital parameters to ensure the accuracy of the sensor in real-time monitoring is the repeatability and the stability of the sensor response.
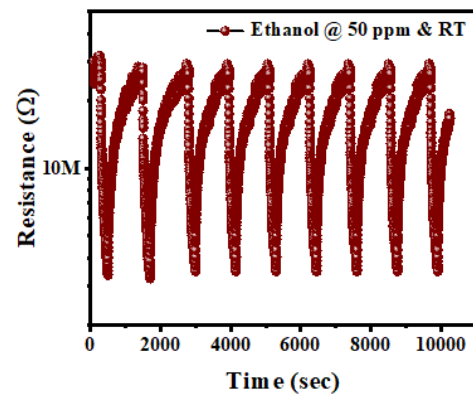
Fig. 5. Dynamic resistance (A), fitting curve between concentration and response (B) and response/recovery time (C) of SnS_2-based gas sensor to various ethanol concentration at RT.

Fig. 6. Nine-cycle repeated resistance curve of the SnS_2-gas sensor to 50 ppm ethanol at RT.

Table 1. Some publications on gas sensors based on 2D materials in detecting VOCs gases.

| Sensing material	Gases	Conc.	Response	Temp (°C)	τ_{res}/ τ_{rec} (s)	Ref.
MoS_2/TiO_2	Ethanol	100 ppm	62 %	350	52/155	[26]
MoS_2/CeO_2	Ethanol	50 ppm	7.78	RT	7.78	[27]
MoS_2/SnO_2	TEA	100 ppm	113.5	200	62/153	[28]
ZnO/MoS_2	acetone	20 ppm	4.67	100	56/69	[29]
MoS_2-CuO	acetone	10 ppm	16.21	RT	61/85	[30]
$MoSe_2$	TMA	100 ppm	4.2	RT	32/25	[31]
1 wt% Au/ PbS-SnS_2	Ethanol	60-1600 ppm	55-120 %	RT	< 80 s	[32]
SnS_2/ZnS	TEA	50 ppm	11.21	180	2/8 s	[33]
SnS_2	acetone	50-1000 ppm	1.6 - 5.2	RT		This work
	ethanol	50-1000 ppm	15 - 49	RT	211/425 (50ppm)	This work
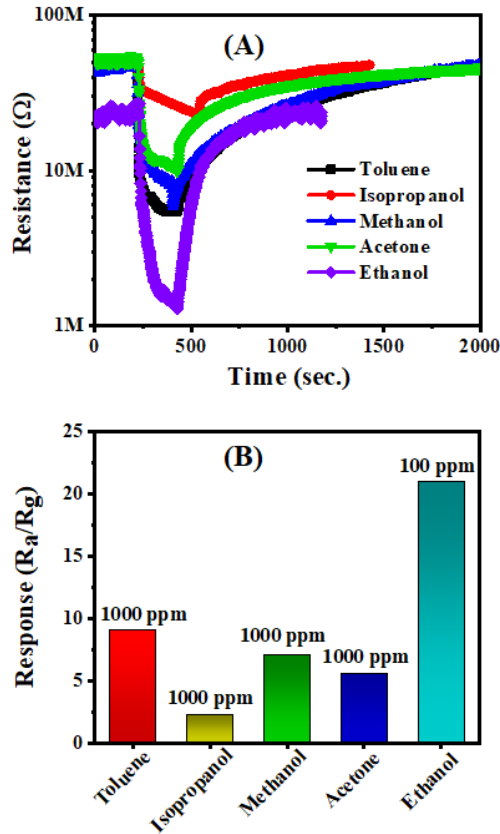
Fig. 7. The resistance curve of SnS$_2$ sensor to 100 ppm ethanol and 1000 ppm various VOCs (i.e, toluene, isopropanol, methanol, and acetone) at room temperature.

The SnS$_2$ sensor was tested for interfering VOCs gases except for ethanol since these gases are present in the practical environment. Fig. 7 (A-B) shows the transient resistance of the sensor to 1000 ppm of other gases including toluene, methanol, acetone, isopropanol, and 100 ppm of ethanol. The resistance tends to decrease after introducing target gases. This reveals that the sensor behaves as an n-type semiconductor when exposure all reducing gas.

In addition, the ultra-thin SnS$_2$ nanosheets-based sensor exhibits a much highest response to 100 ppm ethanol ($R_a/R_g = 20.9$) compared with 1000 ppm other gases. This is attributed to the unique adsorption properties between the physically adsorbed ethanol. The results demonstrate that the SnS$_2$ sensor reaches superior selectivity to ethanol.

3.3. Gas Sensing Mechanism

The sensitive mechanism of stacked hexagonal-structure SnS$_2$ nanosheets is explained via gas adsorption on the material surface and variation of conductivity after occupying the chemical reaction.

Fig. 8 (A) depicts the ethanol molecules transported to the top of SnS$_2$ nanosheets and adsorbed owing to Vander Waals interaction between layer-to-layer.
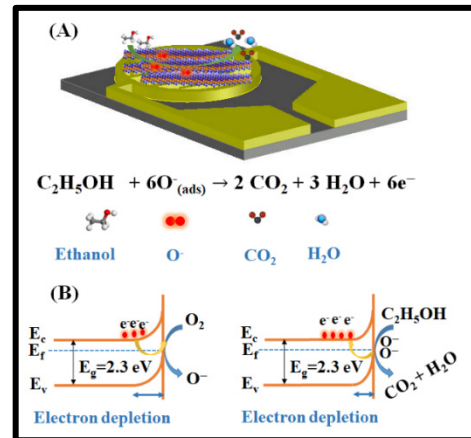

Fig. 8. Scheme of the sensing mechanism (A) Gas adsorption on nanosheets, and (B) Energy band structure of few-layer SnS$_2$ exposed to ethanol gaseous molecules.

First of all, the sensor is placed in the fresh air, the oxygen molecules will be adsorbed on the surface and take an electron from the conduction band to form chemically oxygen species, leading to the electron density tending to decrease and form a depletion layer at the interface between SnS$_2$ material and electrode (Fig. 8B). In this process, the sensor forms Schottky contact due to the greater work function of the Pt electrode (~ 4.9 eV) than the SnS$_2$ one (~2.3 eV), thus the electron transfer from SnS$_2$ to Pt.

This traveling of electron makes the SnS$_2$ have less electron density and form an electron depletion layer at the interface. An increase in potential barrier height is attributed to enhanced gas sensing because of the proportion with actual resistance. Due to the available presence of oxygen species, the adsorption ethanol reacts instantly with negative oxygen ion, resulting in an increase dramatically a quantity of electron carriers on the conductive band, as following equation:

$$C_2H_5OH + 6O^-_{(ads)} \rightarrow 2CO_2 + 3H_2O + 6e^- \quad (2)$$

The electron is released back to the surface of the gas sensor, leading to an increase in the conduction.

4. Conclusion

We have successfully synthesized the ultra-thin SnS$_2$ nanosheets for VOCs gas sensor application. The SnS$_2$ of about 5-layer thickness was prepared by a facile wet chemical method using tin (IV) chloride, oleic acid, octadecene, oleylamine precursors and sulfide was used as sulfidation process. The synthesized SnS$_2$ materials were used to fabricate gas sensors for the detection of toluene, isopropanol, methanol, acetone, and ethanol. The sensor showed the highest response to ethanol, with the response value of 15-50 versus 50-1000 ppm at room temperature. The sensor also exhibited good selectivity and stability.

Acknowledgment

References

[1] World Health Organization, Coronavirus disease 2019 (COVID-19): situation report, 101, 2020.

[2] J. Chen *et al.*, The clinical and immunological features of pediatric COVID-19 patients in China, Genes Dis., vol. 7, no. 4, pp. 535-541, Dec. 2020.
https://doi.org/ 10.1016/j.gendis.2020.03.008.

[3] H. H. Yousef Alimohamadi, Mojtaba Sepandi, Maryam Taghdir, Determine the most common clinical symptoms in COVID-19 patients: a systematic review and meta-analysis, PubMed Cent., vol. 61(3), no. E304-E312, 2020.
https://doi.org/10.15167%2F2421-4248%2Fjpmh2020.61.3.1530.

[4] W. Ibrahim *et al.*, Diagnosis of COVID-19 by exhaled breath analysis using gas chromatography-mass spectrometry, ERJ Open Res., vol. 7, no. 3, pp. 00139-02021, Jul. 2021.
https://doi.org/ 10.1183/23120541.00139-2021.

[5] V. Saasa, T. Malwela, M. Beukes, M. Mokgotho, C.-P. Liu, and B. Mwakikunga, Sensing technologies for detection of acetone in human breath for diabetes diagnosis and monitoring, Diagnostics, vol. 8, no. 1, p. 12, Jan. 2018.
https://doi.org/ 10.3390/diagnostics8010012.

[6] S.-J. Choi *et al.*, Selective diagnosis of diabetes using Pt-Functionalized WO 3 hemitube networks as a sensing layer of acetone in exhaled breath, Anal. Chem., vol. 85, no. 3, pp. 1792-1796, Feb. 2013.
https://doi.org/ 10.1021/ac303148a.

[7] WHO, Air pollution in the Western Pacific. https://bom.so/Cvhx4Z.

[8] J. M. Seguel, R. Merrill, D. Seguel, and A. C. Campagna, Indoor Air Quality, Am. J. Lifestyle Med., vol. 11, no. 4, pp. 284-295, Jul. 2017.
https://doi.org/ 10.1177/1559827616653343.

[9] Dr. Christian Meyer, Overview of TVOC and Indoor Air Quality, pp. 1-11, 2021.

[10] D. E. Schraufnagel *et al.*, Air pollution and noncommunicable diseases, Chest, vol. 155, no. 2, pp. 417-426, Feb. 2019.
https://doi.org/ 10.1016/j.chest.2018.10.041.

[11] K. Dixit, S. Fardindoost, A. Ravishankara, N. Tasnim, and M. Hoorfar, Exhaled breath analysis for diabetes diagnosis and monitoring: relevance, challenges and possibilities, Biosensors, vol. 11, no. 12, p. 476, Nov. 2021.
https://doi.org/ 10.3390/bios11120476.

[12] S. Kumar, V. Pavelyev, P. Mishra, N. Tripathi, P. Sharma, and F. Calle, A review on 2D transition metal di-chalcogenides and metal oxide nanostructures based $NO2$ gas sensors, Mater. Sci. Semicond. Process., vol. 107, p. 104865, Mar. 2020.
https://doi.org/ 10.1016/j.mssp.2019.104865.

[13] Y. Zhang, W. Zeng, and Y. Li, Hydrothermal synthesis and controlled growth of hierarchical 3D flower-like $MoS2$ nanospheres assisted with CTAB and their NO_2 gas sensing properties, Appl. Surf. Sci., vol. 455, pp. 276-282, Oct. 2018.
https://doi.org/ 10.1016/j.apsusc.2018.05.224.

[14] S. Zhao, G. Wang, J. Liao, S. Lv, Z. Zhu, and Z. Li, Vertically aligned $MoS2$/ZnO nanowires nanostructures with highly enhanced NO_2 sensing activities, Appl. Surf. Sci., vol. 456, pp. 808-816, Oct. 2018.
https://doi.org/ 10.1016/j.apsusc.2018.06.103.

[15] D. Gu, X. Li, Y. Zhao, and J. Wang, Enhanced NO_2 sensing of SnO_2/SnS_2 heterojunction based sensor, Sensors Actuators B Chem., vol. 244, pp. 67-76, Jun. 2017.
https://doi.org/ 10.1016/j.snb.2016.12.125.

[16] Y. Lu *et al.*, Au-Pd modified SnS_2 nanosheets for conductometric detection of xylene gas, Sensors Actuators B Chem., vol. 351, p. 130907, Jan. 2022,
https://doi.org/ 10.1016/j.snb.2021.130907.

[17] X. Dong *et al.*, Rational construction and triethylamine sensing performance of foam shaped α-MoO_3@SnS_2 nanosheets, Chinese Chem. Lett., vol. 33, no. 1, pp. 567-572, Jan. 2022.
https://doi.org/ 10.1016/j.cclet.2021.06.022.

[18] Q. X. Zhang, S. Y. Ma, R. Zhang, Y. Tie, and S. T. Pei, Optimization ethanol detection performance manifested by SnS/SnS_2 nanoparticles, Mater. Lett., vol. 258, p. 126783, Jan. 2020.
https://doi.org/ 10.1016/j.matlet.2019.126783.

[19] Acetone - Hazardous Substance Fact Sheet. [Online] Availble:
https://www.nj.gov/health/eoh/rtkweb/documents/fs/0006.pdf.

[20] L. V. Duy, T. T. Nguyet, D. T. T. Le, N. V. Duy, H. Nguyen, F. Biasioli, M. Tonezzer, C. Di Natale, and N. D. hoa, Room temperature ammonia gas sensor based on p-Type-like V2O5 Nanosheets towards food spoilage monitoring, Nanomaterials., vol. 13, pp. 146-163, Dec. 2022.
https://doi.org/ 10.3390/nano13010146.

[21] D. Liu, Z. Tang, and Z. Zhang, Visible light assisted room-temperature NO_2 gas sensor based on hollow SnO_2@SnS_2 nanostructures, Sensors Actuators B Chem., vol. 324, p. 128754, Dec. 2020.
https://doi.org/ 10.1016/j.snb.2020.128754.

[22] S. Singh, S. Raj, and S. Sharma, Ethanol sensing using MoS2/TiO2 composite prepared via hydrothermal method, Mater. Today Proc., vol. 46, pp. 6083-6086, 2021.
https://doi.org/ 10.1016/j.matpr.2020.01.584.

[23] J. Zhang, T. Li, J. Guo, Y. Hu, and D. Zhang, Two-step hydrothermal fabrication of CeO_2-loaded MoS_2 nanoflowers for ethanol gas sensing application, Appl.

Surf. Sci., vol. 568, p. 150942, Dec. 2021. https://doi.org/ 10.1016/j.apsusc.2021.150942.

[24] X. Xu et al., n-n Heterogeneous MoS_2/SnO_2 nanotubes and the excellent triethylamine (TEA) sensing performances, Mater. Lett., vol. 311, p. 131522, Mar. 2022.
https://doi.org/ 10.1016/j.matlet.2021.131522.

[25] X. Chang et al., UV assisted ppb-level acetone detection based on hollow ZnO/MoS_2 nanosheets core/shell heterostructures at low temperature, Sensors Actuators B Chem., vol. 317, p. 128208, Aug. 2020.
https://doi.org/ 10.1016/j.snb.2020.128208.

[26] X. Chang et al., Highly sensitive acetone sensor based on WO_3 nanosheets derived from WS_2 nanoparticles with inorganic fullerene-like structures, Sensors Actuators B Chem., vol. 343, p. 130135, Sep. 2021.
https://doi.org/ 10.1016/j.snb.2021.130135.

[27] N. Hou et al., Fabrication of oxygen-doped $MoSe_2$ hierarchical nanosheets for highly sensitive and selective detection of trace trimethylamine at room temperature in air, Nano Res., vol. 13, no. 6, pp. 1704-1712, Jun. 2020.
https://doi.org/ 10.1007/s12274-020-2796-7.

[28] H. Roshan, P. Salimi Kuchi, M. H. Sheikhi, and A. Mirzaei, Enhancement of room temperature ethanol sensing behavior of $PbS-SnS_2$ nanocomposite by Au decoration, Mater. Sci. Semicond. Process., vol. 127, p. 105742, Jun. 2021.
https://doi.org/ 10.1016/j.mssp.2021.105742.

[29] X. Xu, S. Ma, X. Xu, S. Pei, T. Han, and W. Liu, Transformation synthesis of heterostructured SnS_2/ZnS microspheres for ultrafast triethylamine detection, J. Alloys Compd., vol. 868, p. 159286, Jul. 2021.
https://doi.org/ 10.1016/j.jallcom.2021.159286.

[30] J. Liu, L. Zhang, J. Fan, B. Zhu, and J. Yu, Triethylamine gas sensor based on Pt-functionalized hierarchical ZnO microspheres, Sensors Actuators B Chem., vol. 331, p. 129425, Mar. 2021.
https://doi.org/ 10.1016/j.snb.2020.129425.

[31] L. Sun, Z. Yao, A. A. Haidry, Z. Li, Q. Fatima, and L. Xie, Facile one-step synthesis of TiO_2 microrods surface modified with Cr_2O_3 nanoparticles for acetone sensor applications, J. Mater. Sci. Mater. Electron., vol. 29, no. 17, pp. 14546-14556, Sep. 2018.
https://doi.org/ 10.1007/s10854-018-9589-8.

[32] H.-L. Yu et al., Fabrication of single crystalline WO_3 nano-belts based photoelectric gas sensor for detection of high concentration ethanol gas at room temperature, Sensors Actuators A Phys., vol. 303, p. 111865, Mar. 2020.
https://doi.org/ 10.1016/j.sna.2020.111865.

[33] X.H. Xu, S. Y. Ma, X. L. Xu, S. T. Pei, T. Han, W. W. Liu, Transformation synthesis of heterostructured SnS_2/ZnS microspheres for ultrafast triethylamine detection, J. Alloys Compd., vol. 868, p. 159286, Jul. 2021.
https://doi.org/ 10.1016/j.jallcom.2021.159286.